J Polym Res (2015) 22: 66
DOI 10.1007/s10965-015-0699-1

ORIGINAL PAPER

Synthesis and characterization of supramolecular corrosion inhibitor nanocontainers for anticorrosion hybrid nanocomposite coatings

Sahar Amiri[1] · **Azam Rahimi**[2]

Received: 20 November 2014 / Accepted: 9 March 2015 / Published online: 2 April 2015

Abstract Supramolecular nanocontainers were prepared by forming an inclusion complex (IC) between β-cyclodextrin (β-CD) and a corrosion inhibitor—either 2-mercaptobenzothiazole (MBT) or 2-mercaptobenzimidazole (MBI)—at room temperature or under sonication. These nanocontainers were used to create an anticorrosion coating that releases corrosion inhibitor only upon the initiation of corrosion. The supramolecular nanocontainers were characterized by ^{1}H NMR, XRD, SEM, and FTIR. Differences between the ^{1}H-NMR, FTIR, and XRD spectra of the physical mixtures and the inclusion complex demonstrated the formation of MBT/β-CD and MBI/β-CD supramolecular nanocontainers in the solid phase. Crystals of the β-CD/MBT and β-CD/MBI inclusion complexes adopted head-to-head channel-type and cage-type conformations, respectively.

Keywords Supramolecular nanocontainers · β-Cyclodextrin · 2-Mercaptobenzothiazole · 2-Mercaptobenzimidazole · Inclusion complex · Corrosion inhibitor

Introduction

The development of materials that possess the ability to recover their main function(s) in response to destructive impact is one of most rapidly growing fields of materials science. Protective organic coatings that can autonomously restore their protective function have been developed and are attracting great interest [1, 2]. Currently, the most popular approach to protecting metallic substrates from corrosion is to apply protective polymer coatings. "Smart" anticorrosion coatings contain inhibitor nanocontainers that are uniformly dispersed in a passive coating [3, 4]. These supramolecular nanocontainers slowly release corrosion inhibitor molecules from their cavities. Incorporating such nanocontainers into a hybrid sol–gel system has proven to be an effective method of enhancing corrosion protection [5–9]. Cyclodextrins are known to be effective complexation agents that have the ability to form inclusion complexes (i.e., supramolecular nanocontainers) with various organic guest molecules that fit into the cavity of the cyclodextrin (Fig. 1).

Organic aromatic and heterocyclic compounds are the usual candidates for such inclusion complexation reactions [10, 11]. Cyclodextrin molecules are cyclic oligosaccharides consisting of 6–12 α-D-glucopyranose monomers that are connected at the carbon atoms C1 and C4 to a lipophilic central cavity and a hydrophilic outer surface. A special characteristic of cyclodextrins is their ability to form inclusion complexes with various organic molecules through host–guest interactions with the interior cavity, thus providing a hydrophobic environment for trapping apolar pollutants [12–15]. These inclusion complexes are created through various interactions such as hydrogen bonding, van der Waals interactions, hydrophobic interactions, and electrostatic attraction [2], and these types of bonds alter the photochemical and photophysical properties of the guest molecules. Thus, the physical, chemical, and biochemical properties of guest molecules are modified when they are bound to an inclusion complex, and the range of application of those guest molecules also can be improved [16, 17].

Sahar Amiri is a Assistant professor at Islamic Azad University.

✉ Sahar Amiri
s.amiri@srbiau.ac.ir

[1] Science and Research Branch, Department of Polymer Engineering, Islamic Azad University, P.O. Box 14155-4933, Tehran, Iran

[2] Department of Polymer Science, Faculty of Science, Iran Polymer and Petrochemical Institute, P.O. Box: 14965/115, Tehran, Iran

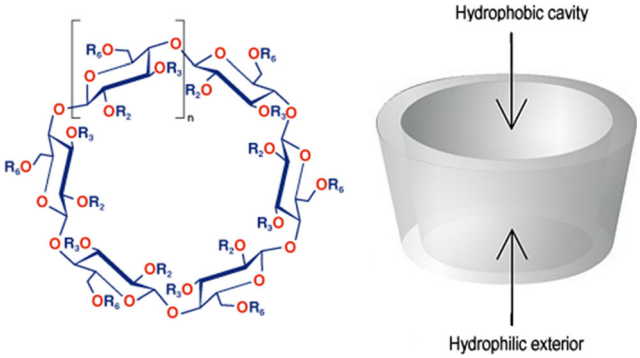

Fig. 1 Molecular structure of cyclodextrins [15]

In the work reported in the present paper, we focused on synthesizing and characterizing corrosion inhibitor nanocontainers obtained via the formation of inclusion complexes of a corrosion inhibitor, either MBI or MBT, with β-cyclodextrin (β-CD) at room temperature and under sonication (it is worth noting that the formation of inclusion complexes of MBI and MBT with α-cyclodextrin has already been investigated [15]). By encapsulating the organic corrosion inhibitors through the formation of inclusion complexes with cyclodextrin and then distributing these inclusion complexes throughout a crosslinked nanoporous coating, we expected to slow down inhibitor leaching, thus prolonging the inhibiting effect of the doping agent. Encapsulating the inhibitors in β-CD molecules was found to provide long-term corrosion protection through the controllable release of corrosion inhibitor, in combination with a secondary chemical equilibrium that was needed to ensure continuous delivery of the inhibitor to corroded sites. The encapsulation of MBT and MBI was demonstrated via FTIR, SEM, ^{1}H NMR, and XRD. The encapsulation of organic corrosion inhibitors as inclusion complexes with cyclodextrin molecules inside a host coating material was found to provide an effective corrosion inhibitor delivery system for active corrosion protection strategies. The slow release of organic corrosion inhibitor molecules from the molecular cavities of cyclodextrin molecules ensures the long-term delivery of inhibitor and thus facilitates corrosion repair over a longer period.

Experimental

Materials

Tetramethoxysilane (TMOS; Aldrich, St. Louis, MO, USA; >98 %), 3-glycidoxypropyltrimethoxysilane (GPTMS; Aldrich; >98 %), 2-mercaptobenzimidazole (MBI; Aldrich; >98 %), 2-mercaptobenzothiazole (MBT; Aldrich; >98 %), diethylenetriamine (EDTA; Aldrich; >98 %), and β-cyclodextrin (β-CD; Applichem, Darmstadt, Germany; 98 %) were used as received. Ethanol was purchased from Merck (Darmstadt, Germany; 98% pure).

Formation of inclusion complexes containing CD/corrosion inhibitors at room temperature

Each inclusion complex of β-CD and a corrosion inhibitor (MBI or MBT) was prepared under two different conditions: with or without sonication. In the approach that did not employ sonication, a solution of the corrosion inhibitor in ethanol (5.0 ml of 14.5 wt %) was added to an aqueous solution of β-CD (5.0 ml of 5.0 wt %). The suspension obtained was stirred at 40 °C for 60 min and then at room temperature for 24 h, after which it was left at room temperature for another 24 h. The resulting solid was collected and then dried at 50 °C in an oven for 24 h. The dried complex was characterized by XRD, SEM, FTIR, and ^{1}H NMR [11, 15, 16].

Formation of inclusion complexes containing CD/corrosion inhibitor under sonication

Each inclusion complex of β-CD and a corrosion inhibitor (either MBI or MBT) was also prepared using sonication. In this approach, a solution of the corrosion inhibitor in ethanol (5.0 ml of 14.5 wt %) was added to an aqueous solution of β-CD (5.0 ml of 5.0 wt %), and the resulting suspension was sonicated in a sonic bath for 60 min at room temperature and then left at room temperature for 24 h. The solid obtained was collected and then dried at 50 °C in an oven for 24 h. The dried complex was characterized by XRD, SEM, FTIR, and ^{1}H NMR [11, 15, 16].

Sol preparation

Hybrid sols were prepared by admixing silica precursors, GPTMS, TMOS, the encapsulated inhibitor, and an organic curing agent, EDTA. GPTMS and TMOS were mixed (in a 2:1 molar ratio) in a beaker with ethanol (12.33 cc) at ambient temperature [17]. The resultant two-phase solution was vigorously stirred at a rate of 240 rpm for 1 h. Water at pH2 was used as an acid catalyst. Hydrolysis and condensation of the silane was conducted at stoichiometric and 50 % substoichiometric water pH2/ethanol ratios in the presence of the acid catalyst. After hydrolysis and condensation, the sol was stirred at room temperature for 2 h [6, 17].

Encapsulated inhibitor was synthesized as reported previously [17]. Encapsulated inhibitor solution (5 % w/w) in ethanol was added to the sol and sonicated for 30 min before a crosslinking agent (diethylenetriamine, DETA, 0.5 ml) was added to the mixture. The final mixture was vigorously stirred and applied onto cleaned 2024 aluminum alloy panels. To prepare these samples for analytical tests, the coated panels were dried under ambient conditions for 24 h.

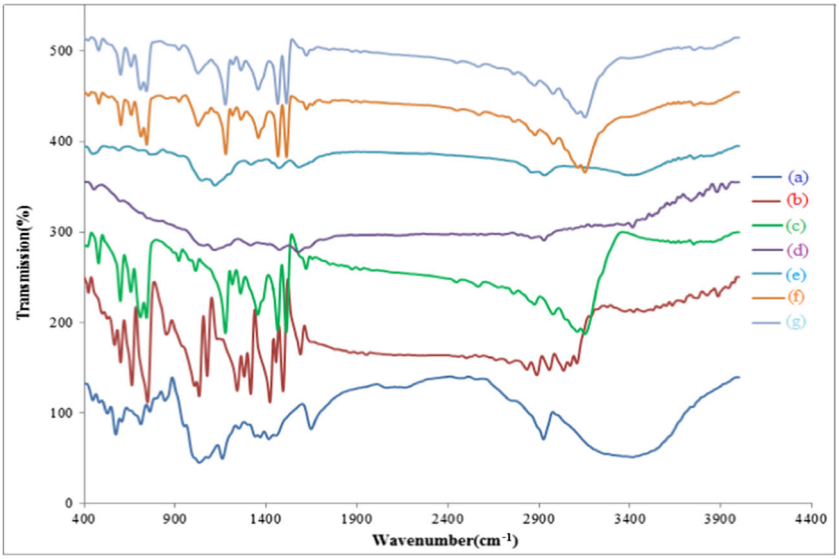

Fig. 2 **a**–**g** FTIR spectra of **a** β-CD, **b** MBT, **c** MBI, **d** β-CD/MBI formed under sonication, **e** β-CD/MBT formed under sonication, **f** β-CD/MBT formed at room temperature without sonication, and **g** β-CD/MBI formed at room temperature without sonication

Electrochemical analysis of the smart corrosion inhibitor nanocontainers

Electrochemical measurements were performed under the extreme environmental conditions created by exposing the samples to an aqueous, air-exposed sodium chloride (5 % NaCl) solution. Each sample was sealed with waterproof tape in order to prevent premature corrosion along the edges of the substrate. A 1 × 1 cm area within the center of each sample was exposed to the solution during testing. Corrosion analysis of

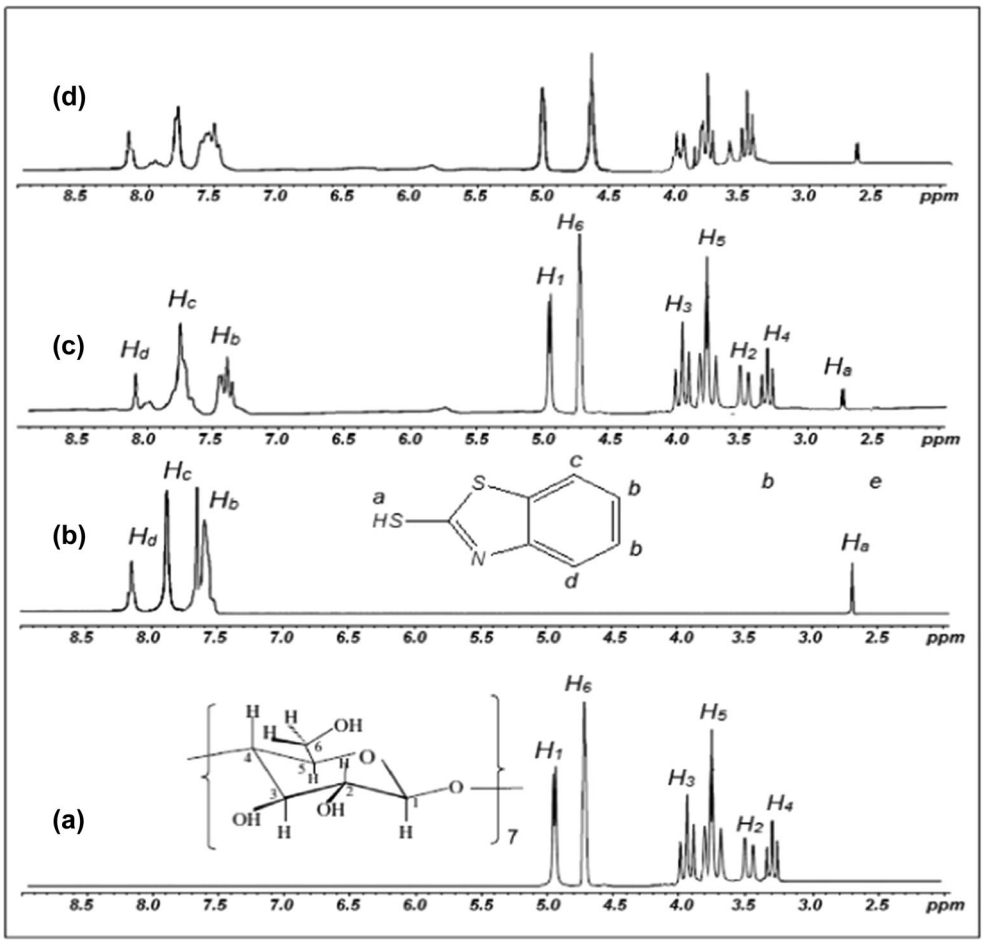

Fig. 3 **a**–**d** ^{1}H NMR spectra of **a** β-CD, **b** MBT, **c** β-CD/MBT formed at room temperature without sonication, **d** β-CD/MBT formed under sonication

bare and coated substrates was performed using an Autolab PGSTAT30 potentiostat system (Metrohm, Utrecht, Netherlands) connected to a corrosion analysis software program. Polarization measurements were carried out potentiostatically at room temperature using an Ag/AgCl/Cl^-(0.222 V) reference electrode and a platinum counter electrode. The potentiodynamic measurements were taken within the range −2000 to 2000 mV versus Ag/AgCl/Cl at a rate of 5 mV/s. Prior to the measurements, in order to reach a steady potential, the electrodes were kept in the working solution for at least 30 min [6].

Corrosion resistance test

The corrosion resistance of each bare or coated aluminum alloy substrate was evaluated by exposing the sample to a salt fog atmosphere generated from a 5 wt% aqueous NaCl solution at 35±1 °C for 2000 h, in accordance with ASTM B117 specifications [6].

Characterization

Solid-state hydrogen nuclear magnetic resonance (^{1}H NMR) spectra were recorded with a Bruker (Rheinstetten, Germany) DRX 500 spectrometer (500 MHz) in deuterated chloroform. Infrared spectra were recorded with a Bruker IFS 48 FTIR spectrometer. X-ray diffraction (XRD) was used to study the diffraction patterns of cyclodextrin/corrosion inhibitor crystals under ambient conditions; an Xpert diffractometer (Philips, Andover, MA, USA) with nickel-filtered Cu Kβ radiation was used in this work. Data were collected at a rate of 2°θ min over the range 2θ=5~60°. Scanning electron microscopy (SEM) using a Philips XL30 was employed to study the Au-coated microstructures of complexes [11, 13, 15].

Results and discussion

When an MBI/ethanol or MBT/ethanol solution was added to an aqueous solution of β-CD and mixed at room temperature

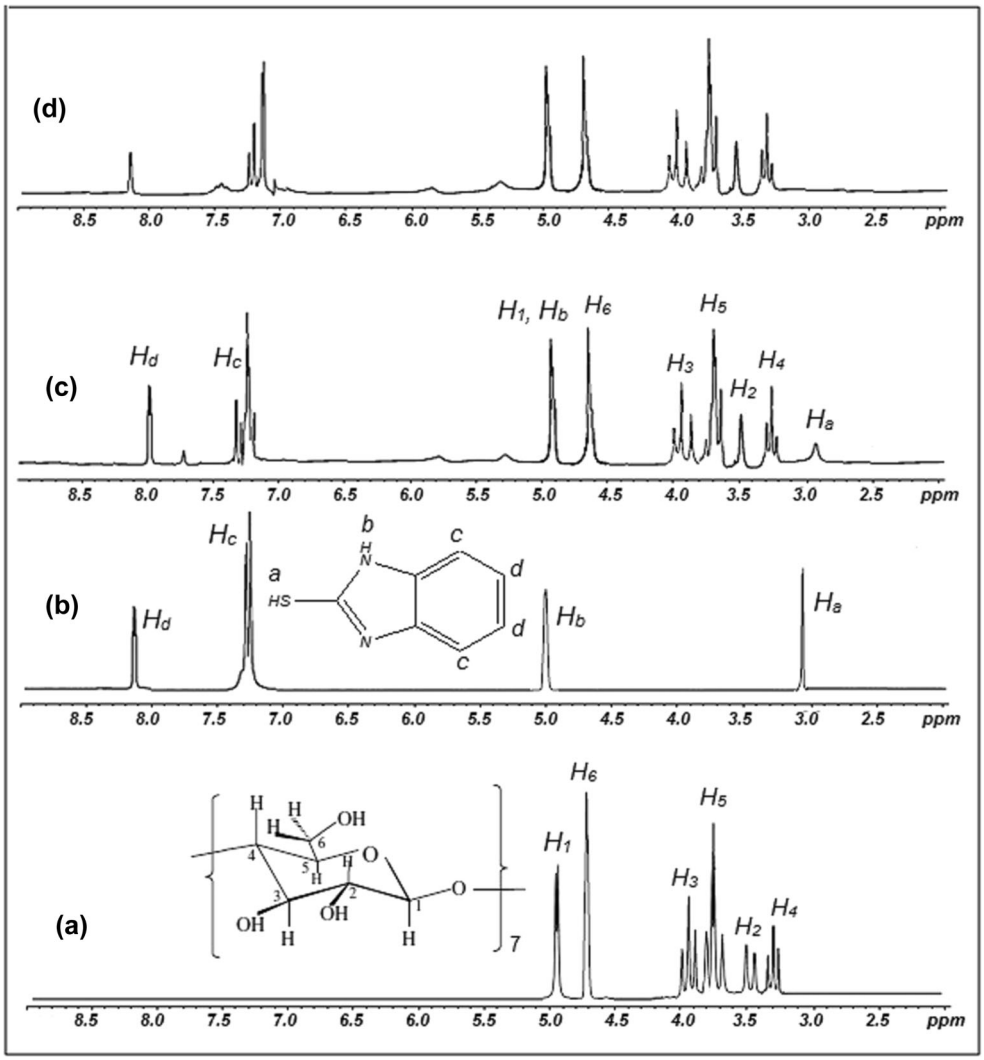

Fig. 4 **a**–**d** ^{1}H NMR spectra of **a** β-CD, **b** MBI, **c** β-CD/MBI formed at room temperature without sonication, **d** β-CD/MBI formed under sonication

or under sonic energy for an appropriate amount of time, the heterogeneous solution became turbid, and—when complex formation was observed—crystalline precipitates of the complexes formed. Different techniques such as FTIR, XRD, and ^{1}H NMR were used to characterize and compare the physicochemical properties of the solid complexes in order to investigate and compare the different preparation methods in terms of their potential and effectiveness [11, 15, 16].

Characterization

The FT-IR technique was used to detect complex formation in the solid phase and to identify the functional groups responsible for the stability of the solid inhibitor/β-CD complex.

IR spectroscopic analysis is a very useful tool for proving the existence of both guest and host molecules in the inclusion complexes [11, 15, 16]. Changes in the IR spectra of a guest molecule and β-CD occur upon the formation of an inclusion complex incorporating both molecules (Fig. 2).

FTIR peaks from β-CD are observed at 3342.72, 2916.53, 1161.84, and 1043.24 cm^{-1}, which correspond to the symmetric and antisymmetric stretching bands ν(O–H), ν(CH_2), and ν(C–C), as well as the bending vibration ν(O–H), respectively. There is a broad absorption band from O–H stretching vibrations at about 3200–3600 cm^{-1}. The spectrum for the inclusion complex looks rather similar to that of pure β-CD. The presence of a benzene ring in an aromatic compound is often determined by searching for an aromatic absorption band due to COH stretching near to 3030 cm^{-1}. Amines and imides exhibit two IR stretching bands: one from NOH stretching and the other from CON stretching. Hydrogen bonding between the N–H groups of imides yields multiple absorption bands at around 3000–3200 cm^{-1} [11, 15–18].

A broad hydroxyl band from pure β-CD at 3370.72 cm^{-1} was found to be narrower in the FTIR spectrum of the inclusion complex, which is a good indication of the formation of the inclusion complex, as this is a common phenomenon observed by many researchers when synthesizing the inclusion complex between β-CD (host) and a guest molecule [15–18]. Thus, the FTIR spectrum strongly supports the formation of MBI/β-CD and MBT/β-CD inclusion complexes. Formation of the inclusion complex shifts the band caused by O–H stretching to a higher frequency in the inclusion complex. A sharp band at 1,261 cm^{-1}, assigned to symmetric C–H deformation in methyl groups, can also be seen in the spectrum for the crystalline inclusion complex, but is absent from the spectrum for the pure β-CD [15, 16].

The formation of inclusion complexes between β-CD and the corrosion inhibitors (MBI and MBT) under various conditions was also checked using ^{1}H NMR, as shown in Figs. 3 and 4. It was possible to assign all of the signals in the ^{1}H NMR spectra to monomers, thus supporting the synthesis of MBI/β-CD and MBT/β-CD inclusion complexes [15, 16]. Inserting a guest molecule into the hydrophobic cavity of β-CD resulted in the chemical shift of guest and host molecules in the ^{1}H NMR spectra [11].

In general, upon the formation of an inclusion complex, large chemical shifts are observed for H_3 and H_5, which are located in the inner cavity of β-CD [11, 15]. The chemical shifts for these protons are slightly higher than those seen for

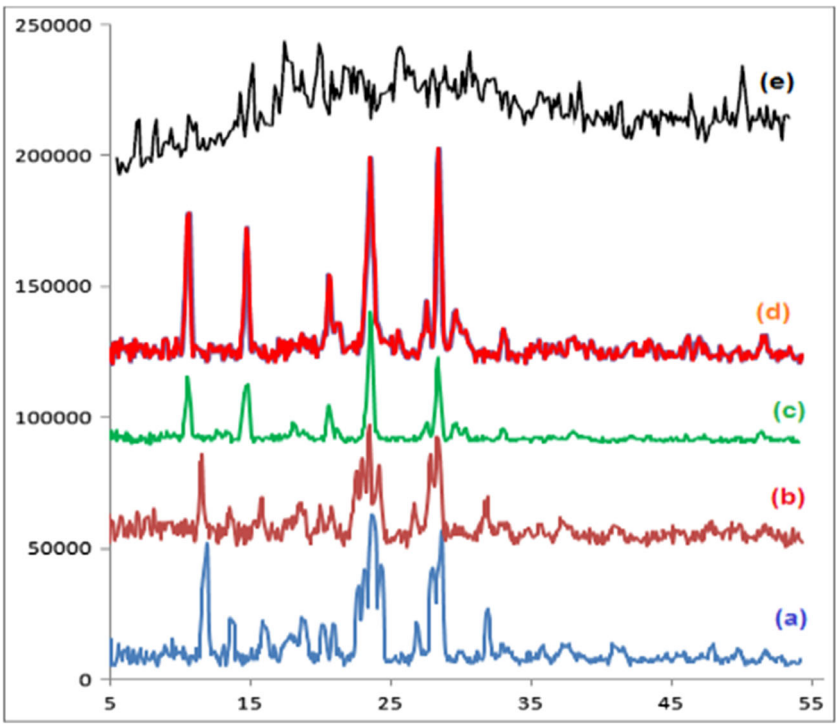

Fig. 5 **a**–**e** XRD spectra of **a** β-CD/MBT formed under sonication, **b** β-CD/MBT formed at room temperature without sonication, **c** β-CD/MBI formed under sonication, **d** β-CD/MBI formed at room temperature without sonication, and **e** β-CD

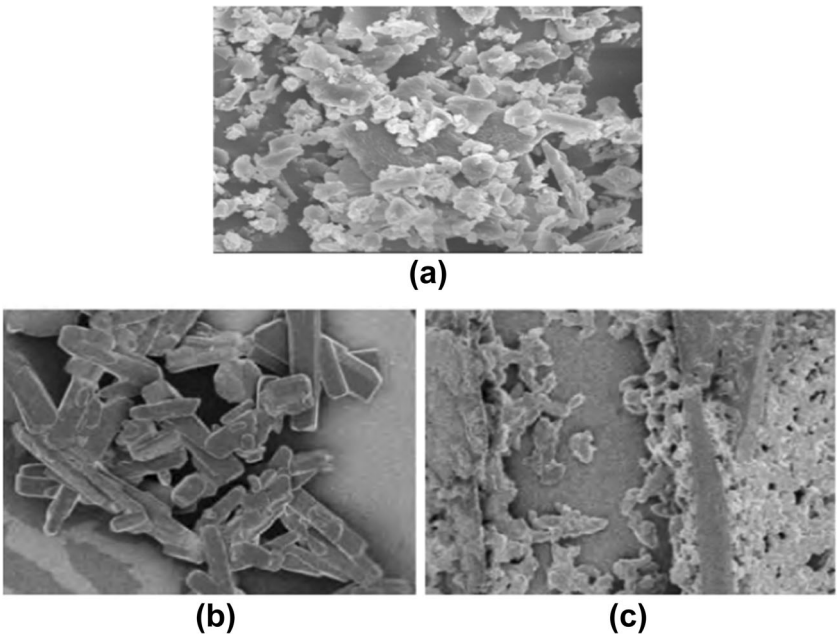

Fig. 6 **a**–**c** SEM images of **a** pure β-CD, **b** pure MBI, and **c** pure MBT at 2 μm

other protons located on the exterior of the cavity. Therefore, these shifts provide further support for the formation of inclusion complexes between β-CD and the inhibitors [17, 18], as also indicated by the FTIR results [17, 18].

More evidence for the formation of inclusion complexes was obtained through X-ray powder diffraction (XRD), as demonstrated in Fig. 5. Basically, there were no visible peaks in the XRD spectrum of pure β-CD, due to the cage-type structure adopted by crystalline β-CD, where the cavity of each β-CD molecule is blocked off on both sides by adjacent β-CD molecules [10–16].

The XRD results confirmed that the inclusion complexes formed are crystalline. Moreover, the appearance of strong peaks at 2θ=12, 23–24, and 28° for the β-CD/MBT inclusion complex suggests that it adopts a head-to-head channel-type structure in the crystalline state, in which the β-CD molecules are stacked along the axis of MBT to form a cylinder (Fig. 5a and b). On the other hand, the strong peaks at 2θ=10, 15, 21 and 23° seen for the β-CD/MBI inclusion complex suggest that this complex adopts a cage-type structure in the crystalline state (Fig. 4c and d) [10, 14].

Supporting evidence for the complexation of MBI or MBT with β-CD and thus the formation of nanocontainers was also obtained by analyzing SEM images. Those for pure β-cyclodextrin, 2-mercaptobenzimidazole, and 2-mercaptobenzothiaole are shown in Fig. 6 at 2 μm [11, 15, 16].

Morphological changes can be used as evidence of interactions between molecules. Figures 7 and 8 show SEM images of MBI/β-CD and MBT/β-CD inclusion-complex formation at room temperature and under sonication, respectively. Thus, the data obtained from SEM supplement previous data suggesting the formation of inclusion complexes of MBT and MBI with β-CD under various conditions, as the shapes and sizes of the particle complexes are completely different from those of the free β-CD (Fig. 6a), MBI (Fig. 6b), and MBT (Fig. 6c) molecules at the same magnification (Figs. 7 and 8). Typical crystals of β-CD, MBI, and MBT show a wide range of sizes. Sonication leads to the more efficient formation of crystalline crystals of the inclusion complexes, as seen in Figs. 7 and 8. Changes in crystal appearance and size are strong indicators of inclusion complex formation [11, 15, 16].

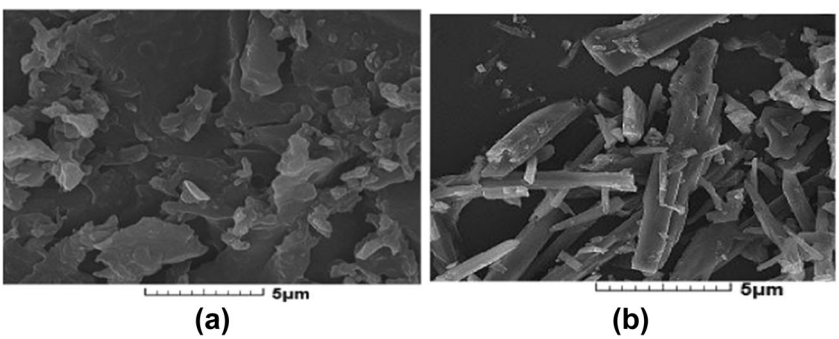

Fig. 7 **a**–**b** SEM images of **a** β-CD/MBT and **b** β-CD/MBI inclusion complexes formed under sonication

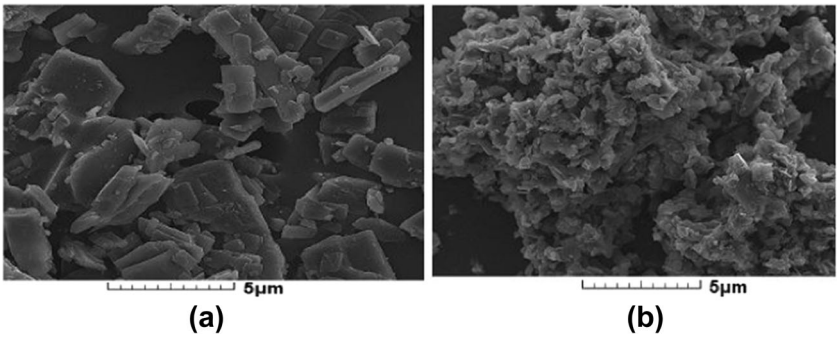

Fig. 8 **a**–**b** SEM images of **a** β-CD/MBT and **b** β-CD/MBI inclusion complexes formed at room temperature without sonication

SEM images showed that discrete homogeneous microcrystals formed under sonication, revealing the significant effect of sonic energy on the formation of supramolecular nanocontainer crystals. In the absence of sonication, the inclusion compounds tended to be formed in a randomized manner—discrete hexagonal homogeneous crystals were not created [15]. The particle size was reduced by applying ultrasonication, and it depended on the treatment time. The shape of the MBI/β-CD inclusion complex crystal was observed to be more ordered than that of the MBT/β-CD inclusion complex crystal, due to the higher content of free hydrogen on MBI and its greater number of hydrogen bonds with cyclodextrin. Hence, the FTIR spectral study and SEM image analysis confirmed the formation of inclusion complexes of MBI and MBT with β-CD [11, 15].

Corrosion inhibitor release mechanism

Water-insoluble thin polymeric films are formed by a surface reaction between cuprous ions and adsorbed inhibitor molecules via a discharge and nucleation mechanism. The resultant film acts as a barrier to corrosion. Cracks and strength decay can be caused by structural changes to atoms or molecules, such as chain scission. Therefore, the inverse reaction—recombination of the broken molecules—represents one of the strategies for repairing corrosion [7, 11]. Reversible self-healing smart materials are more applicable and are able to implement multiple repair cycles via covalent or noncovalent bonding, even when the same site is damaged multiple times. However, a major drawback of self-healing anticorrosion systems based on covalent bonding is the large amount of energy required to break and reform covalent bonds. In contrast, a relatively small amount of energy is needed to break and reform noncovalent bonds, and the encapsulation of a corrosion inhibitor molecule within β-CD is driven by the formation of (reversible and noncovalent) hydrogen bonds. When the nanocontainer is broken or cut, it can be repaired by simply bringing together the fractured ends for just a few minutes at ambient temperature, although is it is crucial to bring the fractured ends of the nanocontainer together as quickly as possible to obtain sufficient self-healing, before the hydrogen-bonding groups at those ends react with other neighboring groups instead [11, 15, 16].

Electrochemical analysis

In complementary experiments, potentiodynamic polarization curves were plotted (Fig. 9) under the extreme environmental conditions generated by an aqueous, air-exposed sodium chloride (5 % NaCl) solution. The potentiodynamic polarization curves in Fig. 9 show that the alloys coated with encapsulated

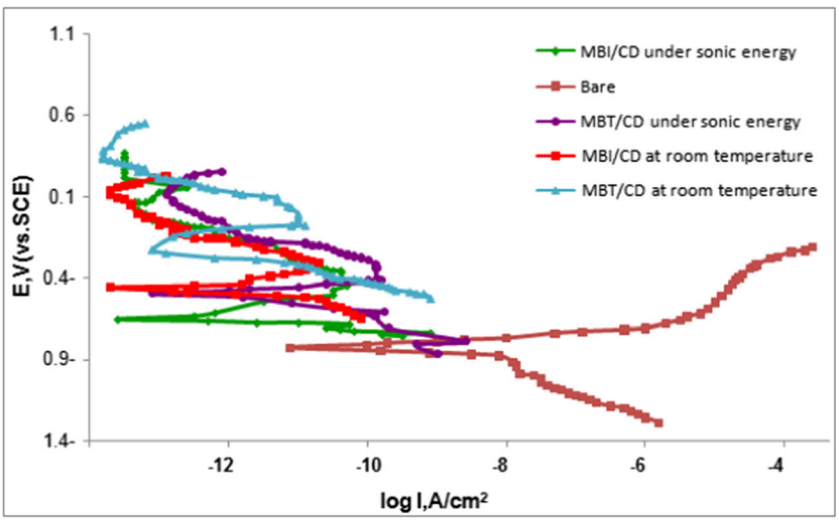

Fig. 9 Potentiodynamic scans of alloys with or without coatings containing inclusion complexes that were formed under different conditions. The scans were performed in dilute 5 % NaCl solution

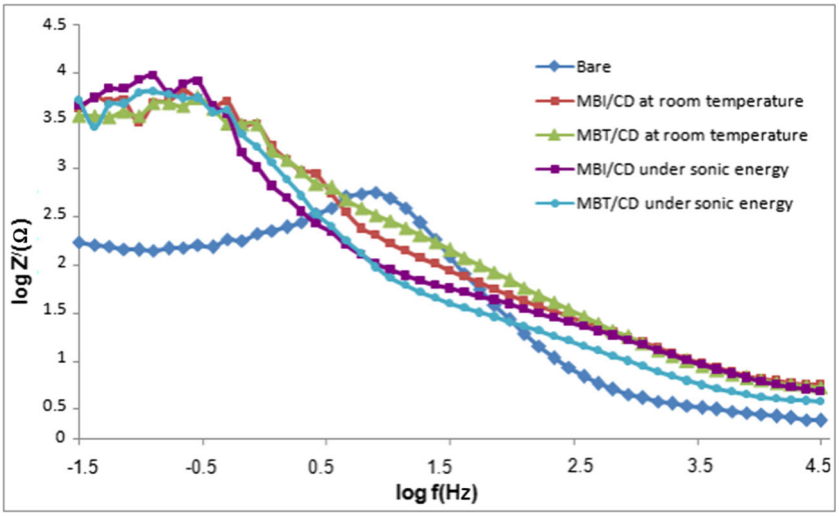

Fig. 10 Electrochemical impedance spectra of scribed alloys with or without coatings containing inclusion complexes that were formed under different conditions. The scans were performed in dilute 5 % NaCl solution

inhibitor coatings showed very different corrosive behavior to that of the alloy with no protective coating (labeled as "Bare" in Figs. 9 and 10). The protected alloys are very resistive: they exhibit very low current density values (in the range from 10^{-14} to 5×10^{-11} A cm^{-2}), which are typical of nonconductive materials such as ceramic coatings. Note that the polarization curves of the coated alloys cover a very wide range of potentials, between −1.4 and 1.1 V versus SCE (2.5 V)—much wider than the potential range observed for the bare alloy [11].

To protect the alloy from corrosion, the corrosion current density must be decreased. The protective coatings containing encapsulated inhibitor molecules that were prepared at room temperature were found to be very effective at passivating and protecting the alloy surface, since the corresponding coated alloys displayed very small current density values in the polarization curves. In contrast, the protective coatings containing encapsulated inhibitor molecules prepared under sonication were found to provide less protection from corrosion [5, 6].

The impedance spectra for the coatings containing MBI/β-CD or MBT/β-CD inclusion complexes along with the spectra for the inhibitor-free sample are shown in Fig. 9. In Table 1, the corrosion rates of the bare and coated alloys are shown; the data indicate that the coating containing MBT/β-CD inclusion complexes provides better protection than the coating containing MBI/β-CD inclusion complexes.

The protection efficiency of a sol–gel coating on an aluminum alloy substrate was calculated as

$$P(\%) = \left(1-\frac{i_{corr}}{i^{o}_{corr}}\right)\times 100,$$

where i^{o}_{corr} and i_{corr} denote the corrosion current densities of the bare and coated electrodes, respectively. The corrosion current density was obtained from the intersection of the anodic and cathodic Tafel lines.

A comparison of these results indicates that both coating systems exhibit similar low-frequency impedance modulus values when initially immersed in the corrosive electrolyte. However, the impedance values for the inhibitor-free coating quickly decrease, indicating that the coating starts to delaminate, which is more likely to happen within the scribed area due to corrosive attack at the coating/substrate interface [5, 6]. Additionally, the alloy substrates coated with inhibitor/cyclodextrin inclusion complexes show much less pitting from corrosion within the scribed area as compared to the alloy with an inhibitor-free coating (Fig. 9). MBT was found to be a more effective corrosion inhibitor than MBI considering differences between the two inhibitors in terms of solubility, the electronic structure of the adsorbed group or atom, and the structure of the inclusion complex.

Table 1 Corrosion protection efficiencies of alloy samples coated with different inhibitor nanocontainers created under different conditions

	Inhibitor nanocontainer			
	MBI/β-CD prepared under sonication	MBI/β-CD prepared at room temperature	MBT/β-CD prepared under sonication	MBT/β-CD prepared at room temperature
Protection efficiency (%)	87.35	96.11	91.41	99.66

Overall, the results of the EIS analysis support our previous conclusion that cyclodextrin-based coating formulations provide effective corrosion protection [5, 6].

Conclusion

In the present paper, we first reported the formation of supramolecular nanocontainers through the generation of β-CD/MBI and β-CD/MBT inclusion complexes under two different conditions (with or without sonication). The formation of these supramolecular nanocontainers was investigated using ^{1}H NMR, SEM, XRD, and FTIR. XRD results indicated the formation of head-to-head channel-type structures and cage-type structures of β-CD/MBT and β-CD/MBI inclusion-complex crystals, respectively. FTIR and ^{1}H NMR spectral studies and SEM image analysis confirmed the formation of inclusion complexes of MBI and MBT with β-CD. These supramolecular nanocontainers proved useful for creating anticorrosion coatings in which the nanocontainers were uniformly distributed in a sol–gel coating. The creation of the inclusion complex of a corrosion inhibitor with cyclodextrin is driven by (reversible) hydrogen-bond formation, which leads to the anticorrosion characteristics of the coating; fractured nanocontainers can be repaired by simply bringing the fractured ends together for just a few minutes at ambient temperature. Hydrogen bonding units may react with the closest ones in their section which is it is crucial to obtain sufficient self-healing property

References

1. Ioannis A, Kartsonakis L, Ioannis L, George Pappas S, George Kordas C (2012) J Nanosci Nanotechnol 10:5912–5920
2. Chen T, Jia Jun J (2012) Nanotechnology 23:505705–505717
3. Khramov AN, Voevodin NN, Balbyshev VN, Donley MS (2004) Thin Solid Films 447–448:549–557
4. Heming W, Robert A (2008) Corros Sci 50:1142–1148
5. Huang M, Zhang H, Yang J (2012) Corros Sci 65:561–566
6. Kumar A, Stephenson LD, Murray JN (2006) Prog Org Coat 55: 244–253
7. Shchukin DG, Zheludkevich M, Yasakau K, Lamaka S, Ferreira MGS, Mohwald H (2006) Adv Mater 18:1672–1678
8. Rajamohan R, Kothai S, Swaminathan NM (2008) Spectrochim Acta A 69:371–377
9. Rajamohan R, Kothai S, Swaminathan NM (2011) J Solut Chem 40:803–817
10. Okumura H, Harada A, Li L, Kawaguchi Y (1993) Macromolecules 26:5698–5703
11. Amiri S, Rahimi A (2014) J Polym Res 21:566. doi:10.1007/s10965-014-0566-5
12. Semsarzadeh MA, Amiri S (2012) Silicon 4:151–156
13. Semsarzadeh MA, Amiri S (2013) Bull Mater Sci 36:989–996
14. Okumura H, Harada A, Li L, Kawaguchi Y (2001) Macromolecules 36:6422–6429
15. Amiri S, Semsarzadeh MA (2013) ACS Symp Ser 1154:87–101
16. Semsarzadeh MA, Amiri S (2013) J Incl Phenom Macrocycl Chem 77:489–499
17. Zandi-zand R, Ershad-langroudi A, Rahimi A (2005) Prog Org Coat 53:286–291
18. PatilDipak R, IngolePravin G, Singh K, DalalDipak S (2012) Res J Chem Sci 2:60–63